Concrete Slab Dynamic Damage Analysis of CFRD Based on Concrete Nonuniformity

Bin Xu[1]; Degao Zou[2]; Xianjing Kong[3]; Yang Zhou, A.M.ASCE[4]; and Xiaoping Liu[5]

Abstract: In general, a concrete slab of a concrete-faced rockfill dam (CFRD) is viewed as a macroscopically uniform but microscopically nonuniform material. Study of the damage process of high CFRD subjected to strong motion is crucial for evaluating its safety during an earthquake. Therefore, dynamic analysis with consideration of the nonuniformity of the concrete should reveal the damage mechanism and provide suggestions for engineering design. In this paper, the elastic–brittle damage model proposed by others and applied to the failure simulation of rock and concrete under static loading was developed for this purpose. The impact of the randomness of the modulus of elasticity and tensile strength of concrete on the distribution characteristics of mechanical damage of the face slab of the rockfill dam was studied. The study considered the randomness of the distribution of material parameters combined with principles of statistics, analyzed using two-dimensional finite-element numerical analysis. The results of the calculation indicate that when the randomness of material parameters of the concrete slab was not considered, the stress of the face slab along the slope direction was larger at ∼0.65–0.85H (H is the dam height) and the tensile damage occurred mainly near 0.8H. As the nonuniformity of the concrete material increased, the location in which tensile damage occurred tended to vary but was concentrated mainly in the ∼0.4–0.9H region of the slab. As a consequence, this part of the face slab is the seismic design focus region. Through the use of elastic–brittle micromechanical damage models and by considering the material parameter randomness, the seismic damage process, damage distribution, and typical damage modes can be intuitively illustrated, which makes it easier to understand the weak points of the slab. The results of this study can provide a reference for the seismic design of CFRD. **DOI: 10.1061/(ASCE)GM.1943-5622.0000939.** *© 2017 American Society of Civil Engineers.*

Author keywords: Concrete-faced rockfill dam (CFRD); Concrete slab; Nonuniformity; Random distribution; Dynamic damage; Micromechanical damage model.

Introduction

A concrete-faced rockfill dam (CFRD) is a type of embankment dam that is being rapidly developed. Compared with core-wall dams, the advantage of CFRDs lies mainly in their better safety and economy and in their ability to adapt to adverse climatic, topographical, and geological conditions. In recent years, along with the rapid development of China's water conservancy, a large number of high rockfill dams have been under construction or design; hydropower dam designs, such as those in Cihaxia and Gushui, have approximated or reached the 300-m dam height level. The construction of high CFRDs has prompted higher requirements for the level of technology used and quality in their construction, especially with the water-prevention structure. The concrete-faced slab is the main water-retaining structure, and its safety and reliability are important for normal operation of the dam.

Concrete is a nonuniform quasi-brittle material with complex mechanical properties. At the microscopic level, it is a nonuniform composite material formed by coarse aggregates, fine aggregates, cement hydrates, unhydrated cement particles, pores, and cracks (Shang and Du 2004), which produce relatively high levels of randomness in the macroscopic mechanical properties. In addition, human factors, such as stirring and transportation during the manufacturing process and pouring during the construction process, also might yield differences in the mechanical properties of the slab at various locations. When a CFRD is analyzed, the face slab is viewed currently as a uniform material and is simulated using a linear elastic model (Zhang 2007). In fact, the linear elastic model can describe only the stress–strain relationship of concrete under low load levels and cannot describe the stiffness degradation and strain-softening characteristics produced by cracking damage. Therefore, it is necessary to use a concrete-damage model that considers the nonuniformity of the material to describe the nonlinear properties of the slab; this approach is especially important for seismic design.

The constitutive model for concrete slabs based on classical mechanical theory usually ignores the nonuniformity of microstructures in concrete and thus has difficulty in describing the mechanical characteristics during the entire concrete-deformation process. Several scholars have conducted a corresponding constitutive relation study from the angle of microstructures using the micromechanics research method combined with theoretical statistics (Ma et

[1]Associate Professor, State Key Laboratory of Coastal and Offshore Engineering and School of Hydraulic Engineering, Dalian Univ. of Technology, Dalian, Liaoning 116024, China (corresponding author). E-mail: xubin@dlut.edu.cn

[2]Professor, State Key Laboratory of Coastal and Offshore Engineering and School of Hydraulic Engineering, Dalian Univ. of Technology, Dalian, Liaoning 116024, China.

[3]Professor, State Key Laboratory of Coastal and Offshore Engineering and School of Hydraulic Engineering, Dalian Univ. of Technology, Dalian, Liaoning 116024, China.

[4]Lecturer, State Key Laboratory of Coastal and Offshore Engineering and School of Hydraulic Engineering, Dalian Univ. of Technology, Dalian, Liaoning 116024, China.

[5]Graduate Student, School of Hydraulic Engineering, Dalian Univ. of Technology, Dalian, Liaoning 116024, China.

Note. This manuscript was submitted on June 30, 2016; approved on February 13, 2017; published online on May 24, 2017. Discussion period open until October 24, 2017; separate discussions must be submitted for individual papers. This paper is part of the ***International Journal of Geomechanics***, © ASCE, ISSN 1532-3641.

al. 2004; Gurson 1977; De Schutter and Taerwe 1993; Dusan and David 1986). Bazant et al. (1990), assuming that the material was composed of spherical particles and considering the randomness of the particle distribution, proposed a random particle model; however, the model ignored the frictional and shear forces between particles. Li (2002) and Li and Chen (2003) used the idea of failure mechanics to propose a concrete random tensile constitutive relation based on random damage evolution; however, the model is complex, with multiple parameters, which renders it difficult to implement. On the basis of the disturbed-state concept (DSC), Desai and Toth (1996) and Desai (2000, 2007, 2010) proposed a constitutive model and developed the unified framework procedure for simulating the behavior of geomaterials and interfaces or joints. In this model, the damage and softening effects of solids could be considered. Tang (1997) and Zhu and Tang (2002) described the problem using an elastic–brittle constitutive relation with residual strength; this established elastic damage model reflects the nonuniformity of the material, is based on the statistical distribution of microcosmic element strength, and is simple and easy to implement. Zhong et al. (2011) used this model to simulate the damage mode of a gravity dam in comparison with the shake table test and obtained results that were in good agreement. Tang et al. (2011) simulated the Koyna dam using a microdamage mechanics model; the simulated dam body damage form is consistent with the actual one. Tian et al. (2010, 2012) established three-dimensional concrete-damage evolution equations using microdamage theory, verified them via a computed tomography scan, and successfully simulated the process of microcrack initiation, expansion, and connection to produce macrocracks in concrete.

However, this analysis involved mainly concrete dam (gravity dam and arch dam) or rock responses. For the CFRD dynamic analysis, few studies in which the nonuniformity of concrete was considered have been reported. First, the concrete-damage model should be used together with the rockfill materials plastic model, and the convergence is difficult to ensure. In addition, the plastic model, considering deformation during the earthquake, should be used for the interface between the slab and the cushion layer. These two factors limit application of the damage model considering the nonuniformity in CFRD dynamic analysis.

In this study, the elastic–brittle damage-analysis method for CFRDs was developed on the basis of the generalized plastic model for rockfill materials (Xu et al. 2012; Liu and Zou 2013) and the generalized plastic interface model between the slab and cushion layer (Liu et al. 2014) established by the authors, extending the elastic–brittle microscopic damage constitutive model with residual strength proposed by Tang (1997), and considering slab nonuniformity induced by factors such as construction and intrinsic material properties. Through a series of two-dimensional finite-element numerical analyses, the characteristics of damage initiation, development, and distribution in a concrete slab under seismic load were examined. The analyses revealed that a significant influence on the damage modes of slabs is observed with different nonuniformities.

Concrete Microcosmic Element Model

Nonuniformity of Concrete

Concrete is a composite material composed of many substances; because of the additional influences from construction techniques, multiple microcracks and voids inevitably exist inside concrete. These defects induce the existence of weak links with different strengths inside concrete, and the mechanical properties (strength, elastic modulus, etc.) of these microcosmic elements are also inconsistent.

To describe the nonuniformity of the material property during the numerical simulation of concrete failure under the loading process, the material characteristics of each microcosmic element are assumed to satisfy a type of random distribution, namely, the Weibull distribution (Weibull 1951). The Weibull distribution is being applied widely in research on reliability and fracture mechanics; it can very well reflect the randomness of material property distribution, and its probability density function is

$$f(x) = \frac{m}{x_0}\left(\frac{x}{x_0}\right)^{m-1} e^{-(x/x_0)^m} \tag{1}$$

where m = degree of uniformity of the material, which reflects the uniformity of the statistical model parameters; $m > 0$; and a higher m value represents a narrower mechanical property distribution and a higher uniformity of the material. As m approaches infinity, the statistical model approaches the ideal uniform distribution; x represents statistical parameters (elastic modulus and tensile strength in this paper), and x_0 is the average value of the statistical parameters. Fig. 1 presents the probability density function versus the x/x_0 curve for concrete and shows that as m increases, the probability density function curve approaches the average value, which indicates that as the degree of uniformity increases, the concrete material approaches uniformity (Mihashi et al. 1991).

The strength of the nonuniformity of the concrete slab is reflected by different degrees of uniformity. To guarantee a sufficient sample size, this method requires a relatively small grid size, ensuring that the sample contains all possible values for the structural elements of the material.

To analyze the influence of the computer-generated random number on the calculation results with the same degree of uniformity, multiple groups of random numbers are taken and the tensile strength distributions in the slabs (FEM mesh is introduced in the "Finite-Element Analysis" section) are compared, as shown in Fig. 2 ($m = 2$). The results indicate that the distributions of tensile strength are basically consistent with the same degree of uniformity.

Fig. 3 shows the curve of the relationship between the number of elements in the slab and the tensile strength at different degrees of uniformity and shows that, as the degree of uniformity m increases,

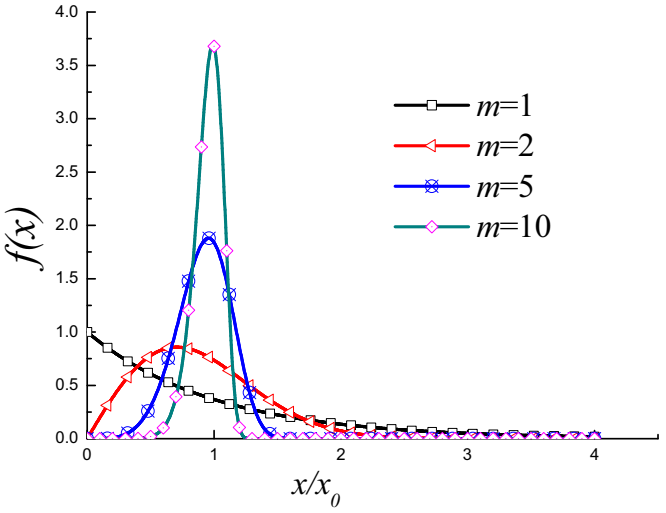

Fig. 1. (Color) Weibull distribution probability density function

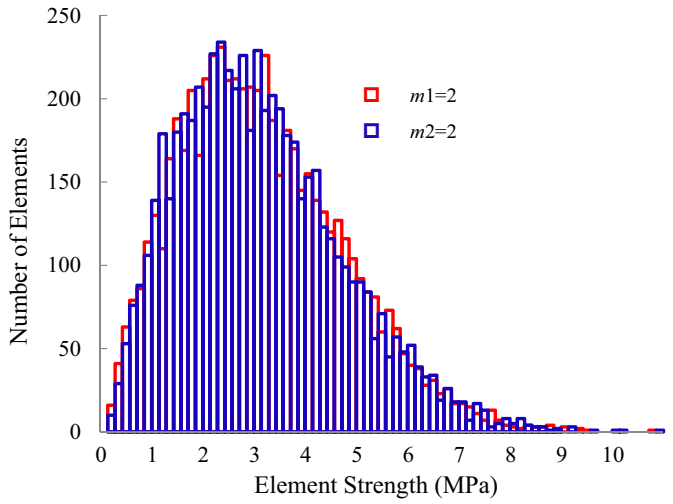

Fig. 2. (Color) Tensile strength distribution in slab elements with $m = 2$

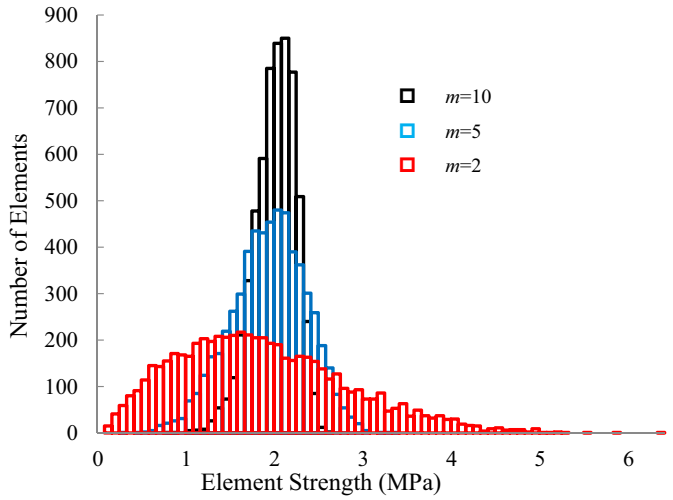

Fig. 3. (Color) Tensile strength distribution in slab elements with different degrees of uniformity

the number of elements that are close to the average strength increases. Fig. 4 shows the contour plot of elastic modulus at different values of m of the concrete slab element; the darker the color is, the higher the element elastic modulus (tensile strength). Because of the current unavailability of relevant reports on material nonuniformity experiments of concrete slab, the degrees of uniformity, m, of the material were chosen to be 2, 5, and 10 for the numerical sensitivity analysis in this paper.

Damage Evolution Equation of Concrete

In general, the strength of the concrete continuously decreases under loading because of damage-induced microcrack initiation and expansion rather than elastic deformation (Ji and Cai 2001). Therefore, it is appropriate to use an elastoplasticity damage constitutive relation to describe the mechanical property of concrete at the microscopic level. According to the strain equivalence principle in damage mechanics

$$\varepsilon = \frac{\sigma}{E_0} = \frac{\bar{\sigma}}{E_0} = \sigma/(1-D)E_0 \tag{2}$$

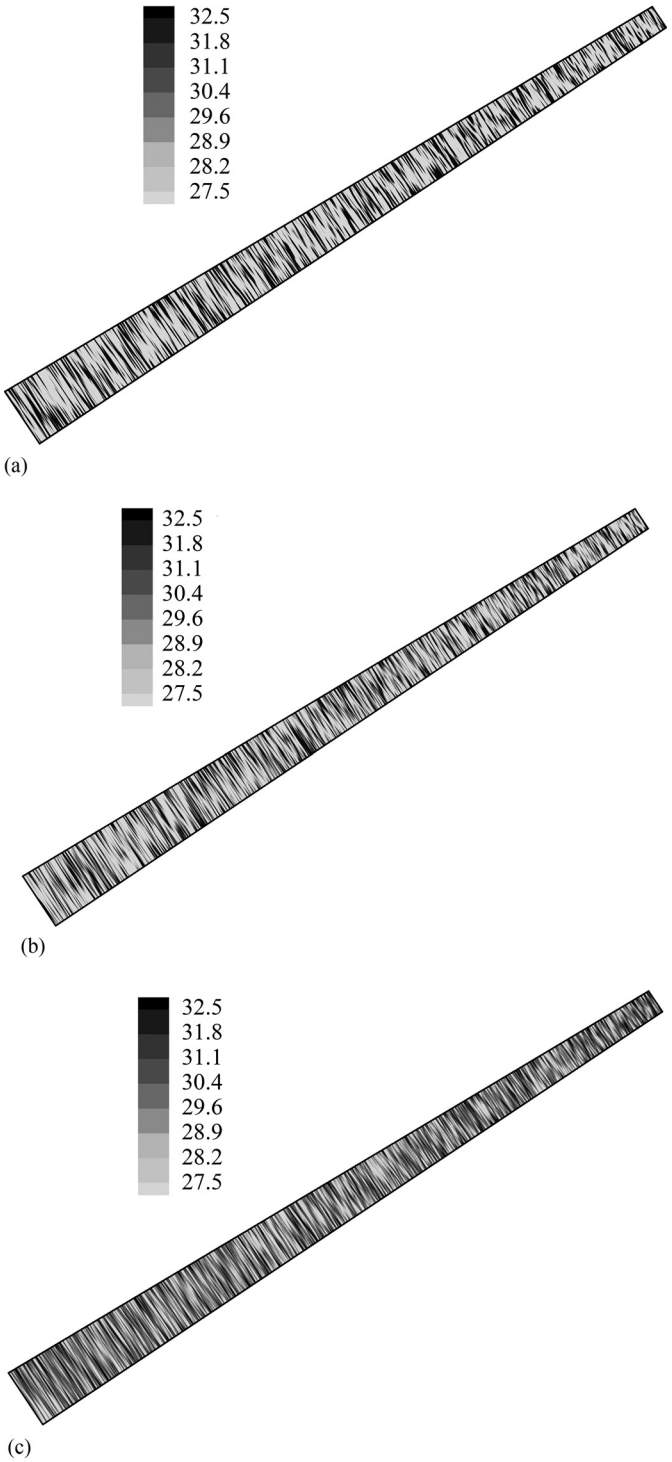

Fig. 4. Contour t of the element elastic modulus with different degrees of uniformity: (a) $m = 2$; (b) $m = 5$; (c) $m = 10$ (Note: Units are gigapascals)

where E_0 = initial elastic modulus; and D = damage variable; $D = 0$ represents the no-damage state, and $D = 1$ represents total damage, which appears macroscopically as cracks. $0 < D < 1$ corresponds to different degrees of damage; in general, $D \geq 0.8$ is viewed as serious damage that has occurred (Lubliner et al. 1989). σ represents nominal stress, and $\bar{\sigma}$ represents effective stress. Under the action of uniaxial tension, the evolution law of tensile damage is as follows in the elastic–brittle model with residual strength:

$$D = \begin{cases} 0 & (\varepsilon \le \varepsilon_{t0}) \\ 1 - \dfrac{\sigma_{rt}}{\varepsilon E_0} & (\varepsilon_{t0} \le \varepsilon \le \varepsilon_{ut}) \\ 1 & \varepsilon \ge \varepsilon_{ut} \end{cases} \quad (3)$$

where σ_{rt} = residual strength and $\sigma_{rt} = \lambda\sigma_t$; ε_{t0} = initial damage threshold, which is the tensile strain corresponding to the limit of elasticity; ε_{ut} = limit of tensile strain; $\varepsilon_{ut} = \eta\varepsilon_{t0}$, where η is the strain coefficient; and λ = residual strength coefficient. The constitutive relation curve under uniaxial tension is shown in Fig. 5.

For the multiaxial loading condition, assuming the damage is still isotropic, the effective strain $\bar{\varepsilon}$ is used to replace ε; $\bar{\varepsilon} = \sqrt{\langle\varepsilon_1\rangle^2 + \langle\varepsilon_2\rangle^2 + \langle\varepsilon_3\rangle^2}$, and ε_1, ε_2, and ε_3 represent principal strains.

When the microcosmic element loading satisfies the Mohr–Coulomb criterion, shear damage will occur; thus, the element can have tensile damage and shear damage simultaneously. The appearance of cracks is mainly a result of tensile action instead of compression, considering that the tensile strength of concrete is much less than the compression strength. Once tensile damage of the element occurs, shear damage is not considered during the calculation process. It was assumed that the concrete would not suffer crushing or compressive damage.

With the tensile strain increasing, damage occurs in the element. The current elastic modulus is expressed as $E = (1 - D)E_0$, so the degradation and softening of stiffness for the damaged elements can be considered. When the maximum tensile strain of the damaged element attains a given ultimate tensile strain, the damaged element is supposed to be totally cracked. Because the mesh size is small, the variation of these elements attained given the ultimate tensile strain can be regarded as crack initiation and propagation. In other words, microcracking and discontinuities in the concrete are illustrated by the macro method.

Validation of the Model and Procedure

The Koyna dam was damaged during a short-duration earthquake (surface wave magnitude, 6.5) on December 11, 1967. Lee and Fenves (1998a, b) proposed a plastic-damage concrete model and used it to simulate the dynamic damage of the dam, and this simulation was used in *Abaqus 6.14* as a typical example of the damage analysis of concrete structures. To validate the proposed model by Tang (1997) and the procedure developed by the authors, the concrete microcosmic element model was used to numericize the Koyna dam earthquake damage and was compared with the results of Lee and Fenves (1998), as shown in Fig. 6. Because of the limited space, the FEM mesh, concrete model parameters, and input seismic waves were not introduced. Detailed information can be found in a paper by Lee and Fenves (1998).

As shown in Fig. 6, the dynamic damage distribution calculated by the model used in this study agrees well with that of Lee and Fenves (1998) in both degree of damage and position of the dam. The results indicate that the procedure developed by the authors can be used to simulate dynamic damage to concrete structures with the concrete microcosmic element model proposed by Tang (1997).

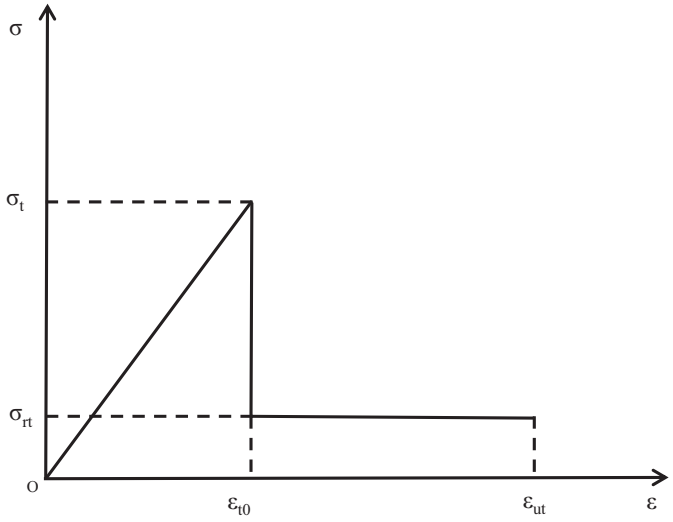

Fig. 5. Tensile element elastic damage constitutive relation curve

Rockfill and Interface Generalized Plasticity Model

Generalized Plasticity Model for Rockfill

The generalized plasticity model (P–Z model) was proposed by Pastor et al. (1985,1990) and Zienkiewicz et al. (1985) on the basis

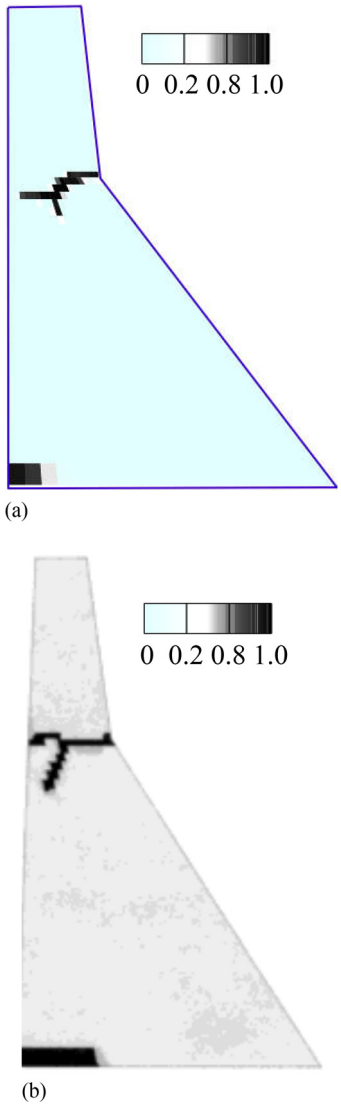

Fig. 6. Comparison of Koyna dam tensile damage distributions at the end of analysis: (a) this paper; (b) Lee and Fenves 1998

of the generalized plasticity theory. The model was focused initially on analyzing the problem of sand liquefaction, and it is suited to geotechnical problems with a small variation in confining pressure (Ling and Liu 2003; Ling and Yang 2006). However, for a high embankment dam, rockfill materials exhibit complex mechanical behaviors, such as strain softening, volume expansion, state-dependent dilation (Xiao et al. 2014b, 2016c), and transitional behaviors (Xiao et al. 2016a), and the average principal stress variation range is ~0–3 MPa. To better describe the high embankment dam deformation characteristics, the correlation of the stress, the state-dependent particle crushing, and dilatancy behaviors of dam construction materials should be considered (Xiao et al. 2014a, 2016b; Kong et al. 2016; Fu et al. 2014). The authors made corresponding improvements to the shear modulus, K, volumetric modulus, G, and loading and unloading modulus, H_{L} and H_{U}, in this generalized plasticity model (Xu et al. 2012; Zou et al. 2013; Kong et al. 2013, 2014).

$$H_{\mathrm{L}} = H_0 P_0 (P/P_a)^{m_1} H_{\mathrm{f}} (H_{\mathrm{v}} + H_{\mathrm{s}}) H_{\mathrm{DM}} H_{\mathrm{den}} \tag{4}$$

$$H_U = \begin{cases} H_{U0} P_0 (P/P_a)^{m_u} (\eta_u/M_g)^{-\gamma_u} & |\eta_{\mathrm{u}}/M_g| < 1 \\ H_{U0} & |\eta_{\mathrm{u}}/M_g| \geq 1 \end{cases} \tag{5}$$

$$K = K_0 (P/P_a)^{m_v} \quad G = G_0 (P/P_a)^{m_s} \tag{6}$$

where H_{L} = plasticity model parameter, $H_f = (1 - \eta/\eta_f)^4$; $\eta_f = (1 + 1/\alpha_f) M_f$; $H_v = 1 - \eta/M_g$; $H_{\mathrm{s}} = \beta_0 \beta_1 \exp(-\beta_0 \xi)$; $\xi = \int |d\varepsilon_{\mathrm{s}}|$; and η, η_f, α_f, M_f, β_0, β_1 = respective calculation model parameters and have the same or similar physical meanings as those in the original model (Pastor et al. 1985, 1990); K_0 and G_0 = initial volume modulus and shear modulus; M_g = slope of the critical state line on the $p-q$ plane; and P_a = standard atmospheric pressure. To better reflect the hysteresis character of the rockfill, the historical function $H_{\mathrm{DM}} = \exp[(1 - \eta/\eta_{\max})_{\mathrm{DM}}]$, in which $\eta_{\max}$ is the historical maximum stress ratio, is modified. The cyclic hardening of the rockfill is considered by modifying the compacting coefficient $H_{\mathrm{den}} = \exp(\gamma_d \varepsilon_v^p)$, where ε_v^p is plastic volumetric strain.

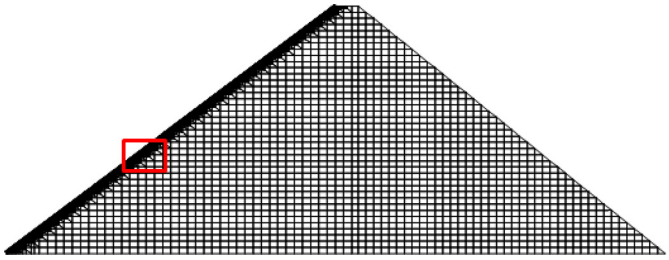

Fig. 7. (Color) CFRD finite-element model

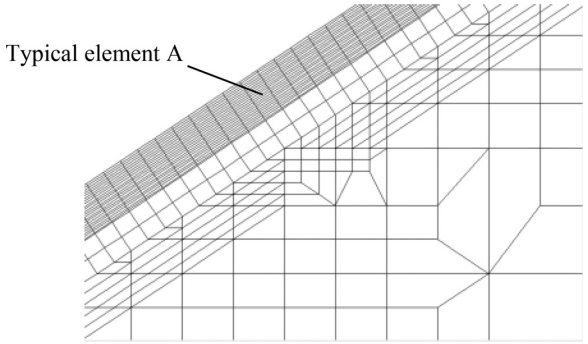

Fig. 8. Magnified face slab and transition layer

Table 1. Generalized Plasticity Model Parameters for Rockfill Materials

Parameter	Value
G_0	1,000
K_0	1,400
M_g	1.8
M_f	1.38
α_f	0.45
α_g	0.40
H_0	1,800
H_{U0}	3,000
m_s	0.5
m_v	0.5
m_1	0.2
m_u	0.2
r_d	105
γ_D	50
γ_u	4
β_0	35
β_1	0.022

Table 2. Generalized Plasticity Contact Surface Model Parameters

Parameter	Value
D_{r0} (kPa)	1,000
D_{n0} (kPa)	1,500
M_g	0.88
λ	0.091
η	0.4
α	0.65
k_m	0.6
γ_d	0.2
k_m	1,000,000
M_f	0.65
H_0 (kPa)	8,500
k_p	0.5
a	5,000
b	1.38
c	0.1
f_h	2.0
e_0	0.25
k_{ts}	100,000

Table 3. Concrete-Faced Slab Parameters

Parameter category	Parameter	Value
Microcosmic element parameters	ρ (kg/m^3)	2,400
	E (MPa)	31
	υ	0.18
	ft (MPa)	3.48
	λ	0.05
	η	10
Degree of uniformity parameters	m_1	2
	m_2	5
	m_3	10

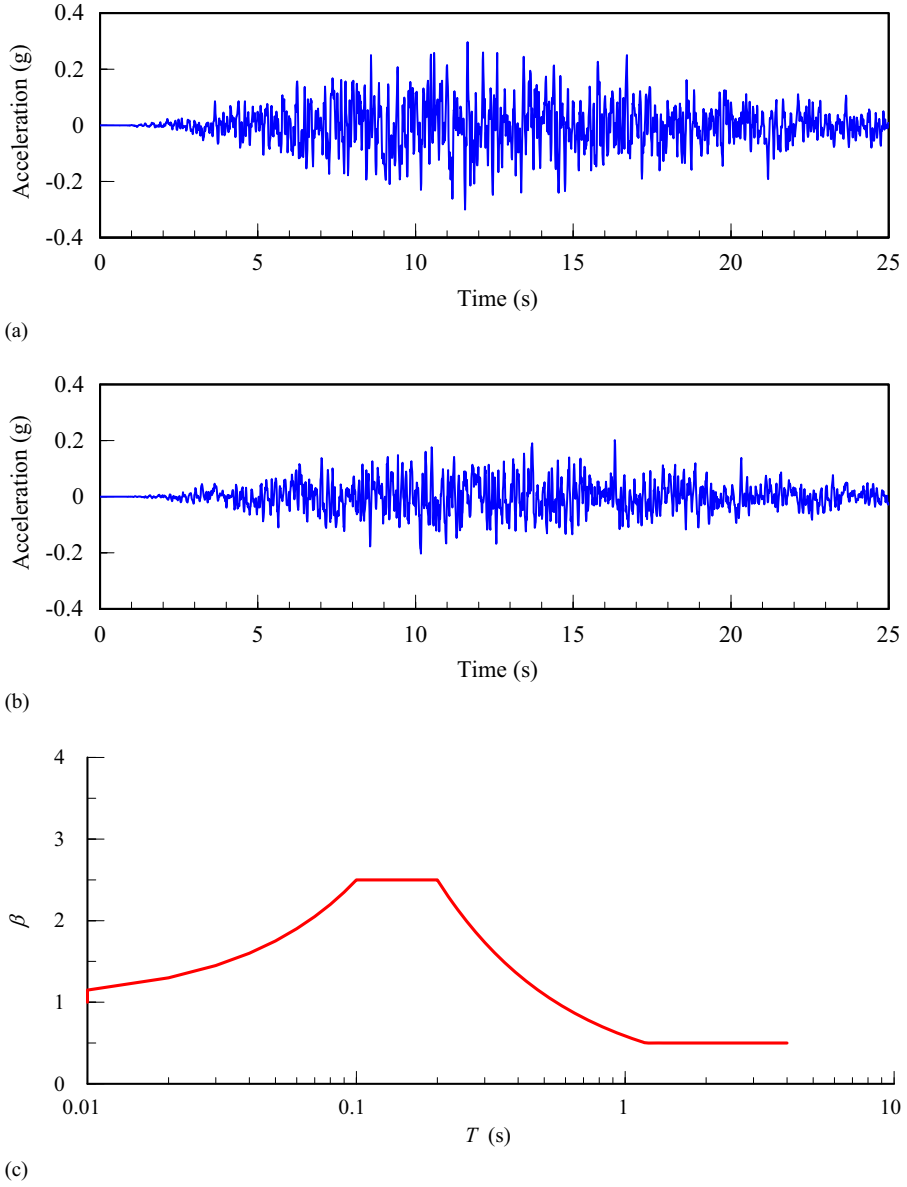

Fig. 9. (Color) Acceleration time-history curves of earthquake with specification spectra (a) along the river direction and (b) in the vertical direction; (c) acceleration amplification-response spectrum

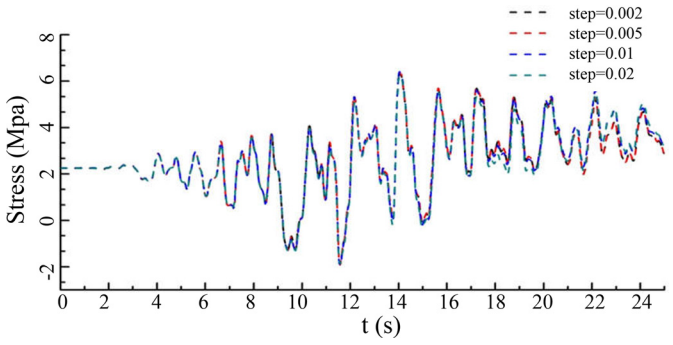

Fig. 10. (Color) Element stress temporal plot with different time-step sizes

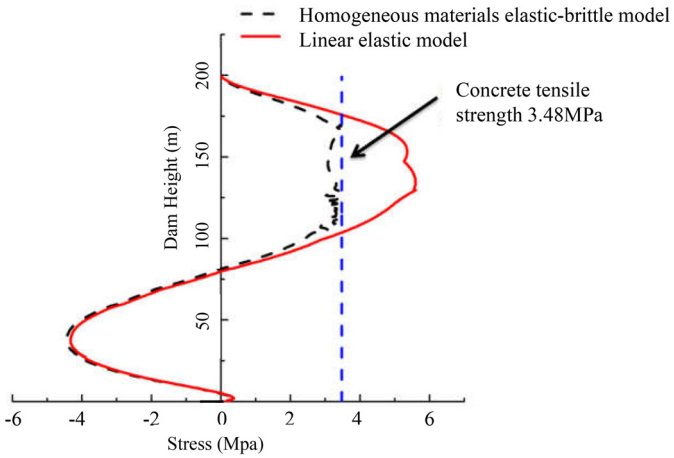

Fig. 11. (Color) Slab stress in the slope direction for different models

Generalized Plasticity Interface Model

The generalized plasticity interface model is an interface model based on the critical state and generalized plasticity framework proposed by Ling and Liu (2003) and Liu and Ling (2006, 2008). However, this model does not provide a unified consideration of the impact of particle breakage under the loading condition. Moreover, when the loading or unloading path passes through locations at which the shear stress is 0, the two types of loading must be distinguished. Liu et al. (2014) used the idea of the boundary surface model (Liu and Zou 2013), a defined peak stress boundary surface, and the maximum historical stress boundary surface within the shear surface to comprehensively consider the impact of particle breakage in the critical state, and an expanded and modified three-dimensional interface model was established.

$$f = \tau - M\sigma_n\left(\frac{\alpha}{\alpha-1}\right)\left[1-\left(\frac{\sigma_n}{\sigma_c}\right)^{\alpha-1}\right] = 0 \tag{7}$$

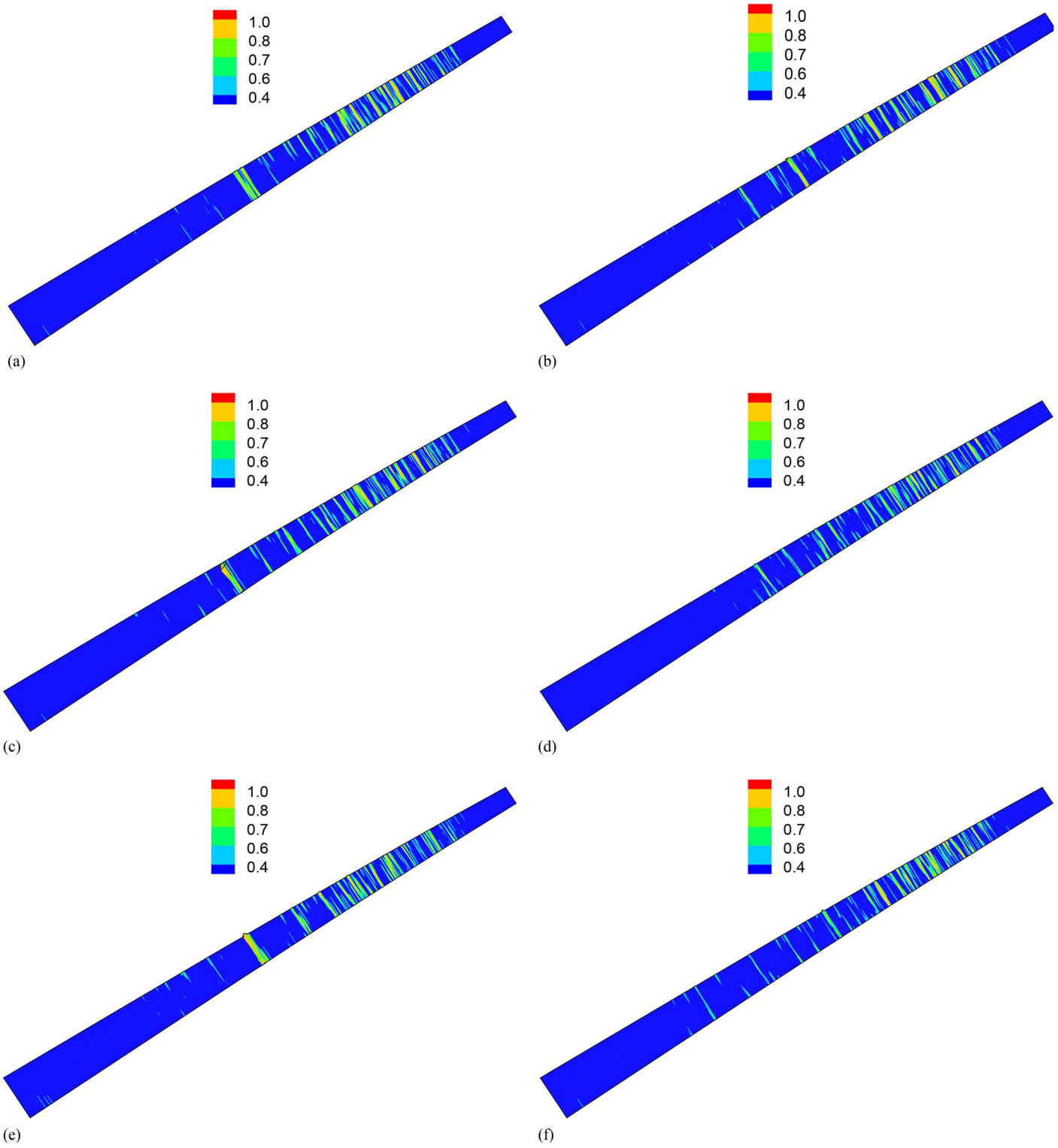

Fig. 12. (Color) Slab tensile damage distribution contour with $m = 2$ (Note: 0 = no damage; 1 = complete damage)

$$e_c = e_{\tau 0} - \Delta e_c - \lambda \ln\left(\frac{\sigma_n}{p_a}\right) \tag{8}$$

$$\Delta e_c = c_3 (B_r)_{\text{virgn}} + c_4 (B_r)_{\text{cyclic}} \tag{9}$$

$$B_r = \frac{W_p}{c_1 + c_2 W_p} \quad dB_r = \frac{-c_1}{(c_1 + c_2 W_p)^2} dW_p \tag{10}$$

in which f = historical maximum stress boundary surface in $\tau - \sigma_n$ space; σ_n = normal direction pressure; α and M = experimental constants; σ_c = yield surface; c_3 and c_4 = different impacts of particle breakage on the critical void ratio under monotonic or cyclic loading, respectively; $(B_r)_{\text{virgn}}$ = particle breakage amount under monotonic loading; and $(B_r)_{\text{cyclic}}$ = particle breakage amount under cyclic loading.

Finite-Element Analysis

Finite-Element Model and Computational Parameters

A two-dimensional concrete-faced rockfill dam with a height of 200 m is used as the finite-element model. The upstream dam slope is 1:1.4, and the downstream dam slope is 1:1.5. The dam is filled in 34 layers, and the face slab is poured in three stages (the slab top heights of each stage are 60, 130, and 200, respectively). The water level is 190 m, and impoundment begins after the second stage of face slab construction.

The finite-element grid of the concrete-faced slab is shown in Fig. 7; the face slab, cushion, and transition layer grid are magnified, with denser grids, in Fig. 8. The face slab is divided into 20 layers along the normal direction; the largest element size is 0.05 m for the convenience of studying the damage development process. The slab element uses four-node isoparametric elements; the interface between the concrete-faced slab and cushion layer uses a four-node Goodman surface element. The thickness of each rockfill layer is less than 5 m. The bottom boundary of the dam was fixed in the x and y directions. The water pressure was simulated as a surface force on the slabs. The model contains 37,989 elements and 37,550 nodes in total, including 24,000 slab elements.

Material Parameters

The parameters of generalized plasticity model for rockfill materials (Xu et al. 2012; Liu and Zou 2013) are listed in Table 1. The generalized plasticity interface model is applied to the interface between the concrete-faced slab and the cushion layer, and the computational parameters (Liu et al. 2014) are listed in Table 2. The reference numeral of the face slab concrete is C30. This paper mainly considers the elastic modulus and nonuniformity of tensile strength; the average values of the material parameters are listed in Table 3.

Input of Seismic Motion

The seismic motion input to the mechanical model is based on specifications for seismic design of hydraulic structures in China (China Water Resources and Hydropower Research Institute 2000) with a specified artificial seismic wave spectrum. The input seismic time histories, together with the amplification-response spectrum, are plotted in Figs. 9(a–c). The peak acceleration of seismic waves along the river direction is 0.3g, and the peak vertical acceleration takes two-thirds of that along the river direction.

Time-Step Sensitivity Test

During the elastic–plastic calculation process, the time step will have a certain impact on the mechanical computational results. Therefore, the results with different time-step sizes are tested with the selected time steps of 0.002, 0.005, 0.01, and 0.02 s. Fig. 10 displays the temporal plot of the stress of typical element A with different time steps. It can be seen that when the time step selected is

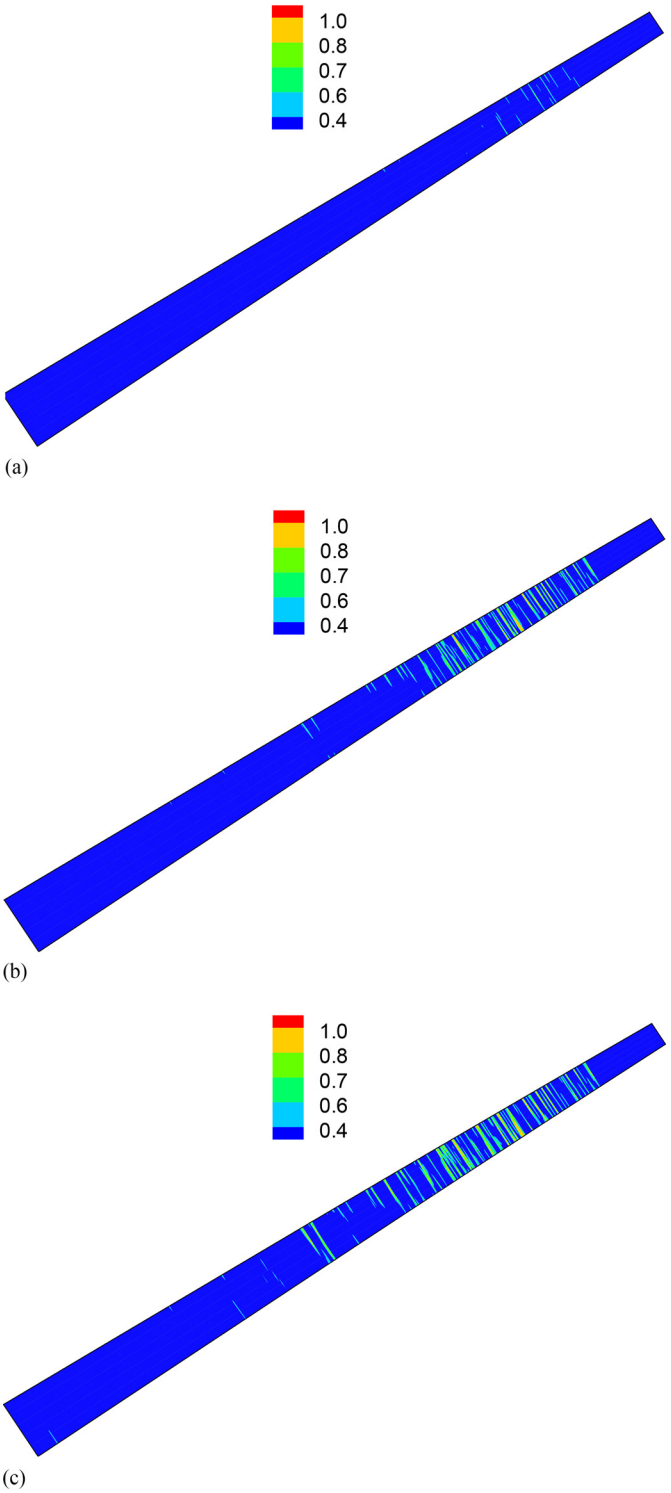

Fig. 13. (Color) Slab-damage development process: (a) t = 9 s; (b) t = 12 s; (c) t = 17 s

0.005 s, the stress histories have slight differences (<2%) from those with a time step of 0.002 s. Fig. 10 shows that the element stress results approach stability when the time step is 0.005 s.

Analysis of Computational Results

The dynamic response of the concrete material is analyzed separately from the linear elastic model and the elastic–brittle damage model. The degree of uniformity m was chosen to be 2, 5, 10, and infinite (homogeneous material) to study the impact of uniformity on the concrete slab damage mode and development process. When it is considered as a homogeneous material, the stress envelope of inner slab layer elements along the slope direction is calculated by using the elastic–brittle damage model and the linear elastic model separately, as shown in Fig. 11. It can be seen that the slab tensile stress along the slope direction within the range of $\sim$0.65–0.85H (H represents the dam height) calculated by the linear elastic model exceeds the concrete tensile strength. By contrast, the elastic–brittle damage model reflects the damage characteristics of concrete when the tensile strength is exceeded; the tensile stress envelope along the slope direction is always smaller than the concrete tensile strength; the computational results are more reasonable.

To eliminate the fortuity of calculation parameters caused by the random distribution function value, 30 cases are calculated for each of the m values of 2, 5, and 10 (in consideration of different uniformity), and each result of the working condition is analyzed. Because of space limitations, this paper uses only $m = 2$ as an example to show the six sets of postseismic slab damage distribution, as shown in Fig. 12. It can be seen that when $m = 2$, the slab elements satisfy the same random distribution; although the damage processes are quite different, the overall postseismic slab damage locations and severities are approximately the same. The damages occur mainly within the range of $\sim$0.4–0.9H, which is consistent with the tensile stress distribution characteristics shown in Fig. 11.

Fig. 13 shows the slab damage development process with $m = 2$. The damage development reveals that the damage first occurs in the 0.8H range of the slab and then gradually expands toward the middle lower portion. As a result of the effect of frictional force, relatively serious tensile damage occurs at the contact region between the concrete slab and cushion layers first and then expands to the slab surface layer.

Fig. 14 shows the postseismic slab damage distribution with different uniformities. It is evident that the lower the uniformity, the more diverse the damaged location will be, mainly because when the uniformity is low, the nonuniformity of the material increases and there are numerous weak links under load in the slab; the tensile stress will reach the tensile strength of a higher number of slab elements under the effect of a seismic load, and tensile damage will occur. By contrast, as the uniformity increases, the material characteristics approach those of a uniform material, the tensile strengths

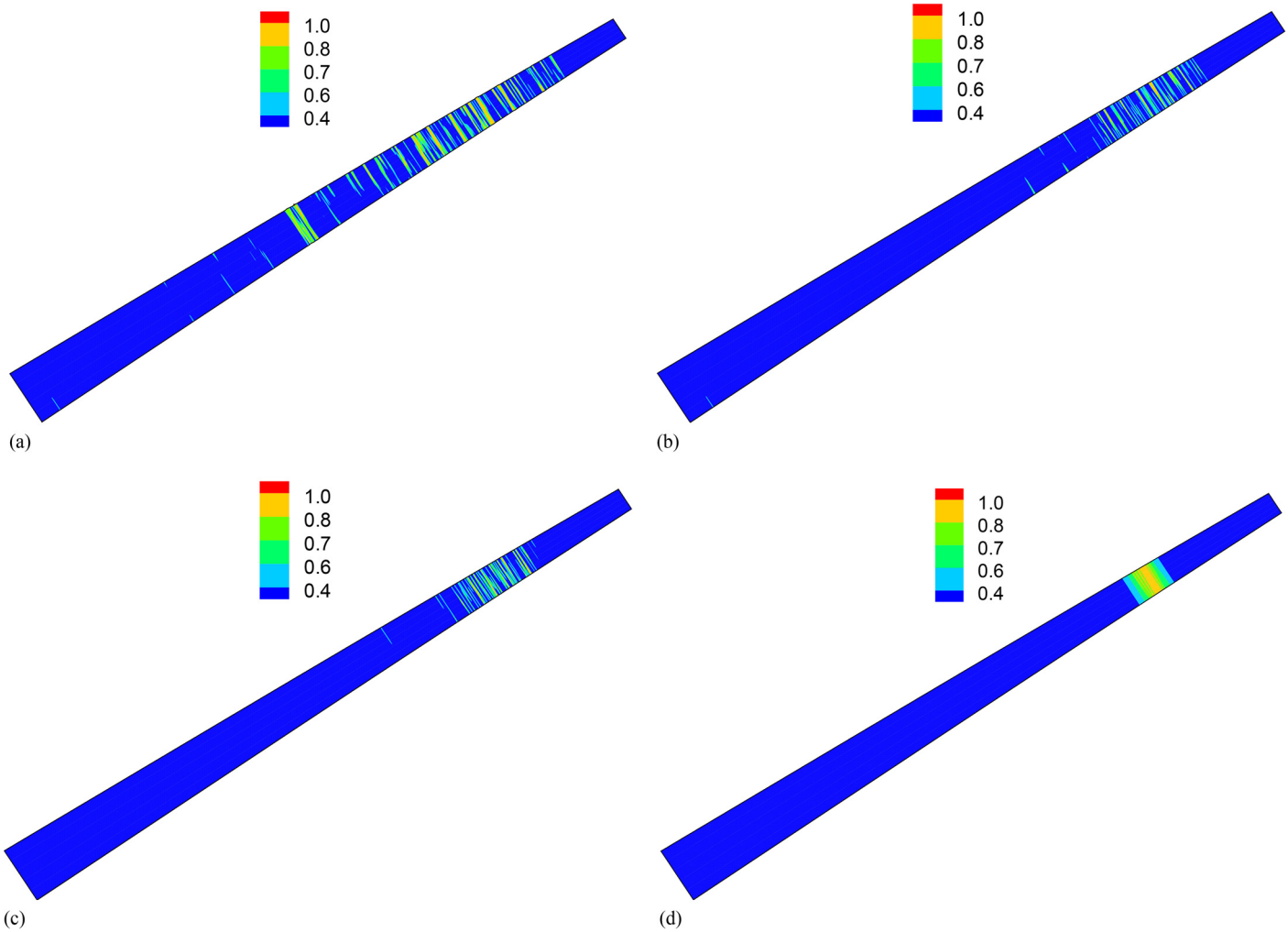

Fig. 14. (Color) Slab damage with different uniformities: (a) $m = 2$; (b) $m = 5$; (c) $m = 10$; (d) homogeneous material (m is infinite)

of each element are close, and the tensile strengths of the elements are relatively large. Under the effect of seismic load, the rockfill body near the dam top has a large displacement, which induces relatively high tensile stress in the region (∼0.65–0.85H); furthermore, tensile damage occurs in the region.

Conclusions

The process of concrete slab pouring is a large-volume concrete construction, and it is very difficult to achieve complete uniformity and ensure complete consistent material properties of the concrete slab. Traditional finite-element analysis for a rockfill dam views the face slab as a uniform material and ignores the nonuniformity of the microscopic structure inside the concrete; thus, it is difficult to describe the mechanical characteristics of the slab during the deformation process. By applying principles of micromechanics and statistics, this study demonstrated a mechanical damage analysis method that takes the randomness of concrete slab material parameters into account.

The elastic–brittle microscopic damage constitutive model by Tang (1997) was extended for the CFRD dynamic analysis. Considering the nonuniformity induced by factors such as concrete slab construction technology and intrinsic material properties, a two-dimensional analysis of a 200-m CFRD was conducted. The impact of randomness in the concrete elastic modulus and tensile strength on the concrete slab damage was studied. The damage process and modes of the slab were investigated.

A sensitivity analysis of material parameter randomness produced by different degrees of uniformity was conducted. The results indicate that under the same degree of uniformity, the location and severity of slab damage are basically the same.

Under a seismic load, the lower the concrete material uniformity degree, the more diverse the locations of slab damage tend to be. The area in which serious damage occur enlarges but is concentrated mainly in the range of ∼0.4–0.9H along the dam height; therefore, this region is the focus area of concrete slab antiseismic design (Xu et al. 2015).

This work is the first to explore the numerical simulation method of dynamic damage of a CFRD slab while considering the nonuniformity of concrete. As a consequence, the damage model and the preferable consideration method of the nonuniformity in the analysis procedure for CFRD need further improvement and verification by comparison with in situ statistical data and laboratory experiment results. These limitations should be clarified progressively in further research.

Acknowledgments

This study was jointly supported by the National Natural Science Foundation of China (Grants 51421064, 51679029, 51379028, and 51508071). The authors greatly acknowledge all this financial support and express their sincerest gratitude.

References

Abaqus [Computer software]. Simulia, Providence, RI.

Bazant, Z., Tabbara, M., Kazemi, M., and Pijaudier-Cabot, G. (1990). "Random particle model for fracture of aggregate or fiber composites." *J. Eng. Mech.*, 10.1061/(ASCE)0733-9399(1990)116:8(1686), 1686–1705.

China Water Resources and Hydropower Research Institute. (2000). "Code for seismic design of hydraulic structures of hydropower project." *DL5073-2000*, China Electric Power Press, Beijing (in Chinese).

De Schutter, G., and Taerwe, L. (1993). "Random particle model for concrete based on Delaunay triangulation." *Mater. Struct.*, 26(2), 67–73.

Desai, C. S. (2000). "Evaluation of liquefaction using disturbed state and energy approaches." *J. Geotech. Geoenviron. Eng.*, 10.1061/(ASCE)1090-0241(2000)126:7(618), 618–631.

Desai, C. S. (2007). "Unified DSC constitutive model for pavement materials with numerical implementation." *Int. J. Geomech.*, 10.1061/(ASCE)1532-3641(2007)7:2(83), 83–101.

Desai, C. S. (2010). "Constitutive modeling and computer methods in geotechnical engineering." *Acta Geotech. Slovenica*, 7(1), 5–29.

Desai, C. S., and Toth, J. (1996). "Disturbed state constitutive modeling based on stress-strain and nondestructive behavior." *Int. J. Solids Struct.*, 33(11), 1619–1650.

Dusan, K., and David, F. (1986). "A micromechanical damage model for concrete." *Eng. Fract. Mech.*, 25(5), 585–596.

Fu, Z. Z., Chen, S. S., and Peng, C. (2014). "Modeling cyclic behavior of rockfill materials in a framework of generalized plasticity." *Int. J. Geomech*, 10.1061/(ASCE)GM.1943-5622.0000302, 191–204.

Gurson, A. L. (1977). "Continuum theory of ductile rupture by void nucleation and growth: Part I-yield criteria and flow rules for porous ductile media." *J. Eng. Mater. Tech.*, 99(1), 297–300.

Ji, H. G., and Cai, M. F. (2001). "Application of acoustic emission technique to predict unstable fracture in concrete." *China Civil Eng. J.*, 34(5), 15–19 (in Chinese).

Kong, X. J., Liu, J. M., Zou, D. G., and Liu, H. B. (2016). "Stress-dilatancy relationship of Zipingpu gravel under cyclic loading in triaxial stress states." *Int. J. Geomech.*, 10.1061/(ASCE)GM.1943-5622.0000584, 04016001.

Kong, X. J., Xu, B., and Zou, D. G. (2014). "Finite element dynamic analysis for seismic damage of slabs of CFRD." *Chin. J. Geotech. Eng.*, 36(9), 1594–1600 (in Chinese).

Kong, X. J., Zou, D. G., Xu, B., Zhou, Y., and Liu, J. M. (2013). "Three dimensional finite element elasto-plastic analysis of Zipingpu concrete faced rockfill dam." *J. Hydroelectr. Eng.*, 32(2), 213–222 (in Chinese).

Lee, J., and Fenves, L. G. (1998a). "Plastic-damage model for cyclic loading of concrete structures." *J. Eng. Mech*, 10.1061/(ASCE)0733-9399(1998)124:8(892), 892–900.

Lee, J., and Fenves, L. G. (1998b). "A plastic-damage concrete model for earthquake analysis of dams." *Earthquake Eng. Struct. Dyn.*, 27(9), 937–956.

Li, J. (2002). "Recent research progress on the stochastic damage constitutional law of concrete." *J. Southeast Univ.*, 32(5), 750–755 (in Chinese).

Li, J., and Chen, J. B. (2003). "The probability density evolution method for analysis of dynamic nonlinear response of stochastic structures." *Acta Mech. Sin.*, 35(6), 716–722 (in Chinese).

Ling, H. I., and Liu, H. B. (2003). "Pressure-level dependency and densification behavior of sand through generalized plasticity model." *J. Eng. Mech*, 10.1061/(ASCE)0733-9399(2003)129:8(851), 851–860.

Ling, H. I., and Yang, S. (2006). "Unified sand model based on the critical state and generalized plasticity." *J. Eng. Mech.*, 10.1061/(ASCE)0733-9399(2006)132:12(1380), 1380–1391.

Liu, H. B., and Ling, H. I. (2008). "Constitutive description of interface behavior including cyclic loading and particle breakage within the framework of critical state soil mechanics." *Int. J. Numer. Anal Methods Geomech.*, 32(12), 1495–1514.

Liu, H. B., and Zou, D. G. (2013). "Associated generalized plasticity framework for modeling gravelly soils considering particle breakage." *J. Eng. Mech.*, 10.1061/(ASCE)EM.1943-7889.0000513, 606–615.

Liu, J. M., Zou, D. G., and Kong, X. J. (2014). "A three-dimensional state-dependent model of soil-structure interface for monotonic and cyclic loadings." *Comput. Geotech.*, 61(Sep), 166–177.

Lubliner, J., Oliver, J., Oller, S., and Oñate, E. (1989). "A plastic-damage model for concrete." *Int. J. Solids Struct.*, 25(3), 299–326.

Ma, H. F., Chen, H. Q., and Li, B. K. (2004). "Meso-structure numerical simulation of concrete specimens." *J. Hydraul. Eng.*, 35(10), 27–35 (in Chinese).

Mihashi, H., Nomura, N., and Niiseki, S. (1991). "Influence of aggregate size on fracture process zone of concrete detected with three dimensional acoustic emission technique." *Cem. Concr. Res.*, 21(5), 737–744.
Pastor, M., Zienkiewicz, O. C., and Chan, A. H. C. (1990). "Generalized plasticity and the modelling of soil behaviour." *Int. J. Numer. Anal. Methods Geomech.*, 14(3), 151–190.
Pastor, M., Zienkiewicz, O. C., and Leung, K. H. (1985). "Simple model for transient soil loading in earthquake analysis. II. Non-associative models for sands." *Int. J. Numer. Anal. Methods Geomech.*, 9(5), 477–498.
Shang, Y., and Du, C. B. (2004). "Advances in numerical simulation of mechanical performance of concrete based on micro-mechanics damage." *J. Water Resour. Archit. Eng.*, 1(2), 23–27.
Tang, C. A. (1997). "Numerical simulation of progressive rock failure and associated seismicity." *Int. Rock Mech. Min. Sci.*, 34(2), 249–261.
Tang, X., Zhou, Y., Zhang, C., and Shi, J. (2011). "Study on the heterogeneity of concrete and its failure behavior using the equivalent probabilistic model." *J. Mater. Civ. Eng.*, 10.1061/(ASCE)MT.1943-5533, 0000179.
Tian, W., Dang, F., and Chen, H. (2010). "3D numerical simulation of concrete failure process and CT verification based on meso-damage." *Rock Soil Mech.*, 31(6), 428–433 (in Chinese).
Tian, W., Dang, F., and Chen, H. (2012). "Fractal analysis on meso-fracture of concrete based on the technique of CT image processing." *J. Basic Sci. Eng.*, 20(3), 424–430 (in Chinese).
Weibull, W. (1951). "A statistical distribution function of wide applicability." *J. App. Mech.*, 18(3), 293–297.
Xiao, Y., Coop, M., Liu, H., Liu, H. L., and Jiang, J. S. (2016a). "Transitional behaviors in well-graded coarse granular soils." *J. Geotech. Geoenviron. Eng.*, 10.1061/(ASCE)GT.1943-5606.0001551, 06016018.
Xiao, Y., Liu, H., Chen, Y., and Jiang, J. S. (2014a). "Strength and deformation of rockfill material based on large-scale triaxial compression tests. II: Influence of particle breakage." *J. Geotech. Geoenviron. Eng.*, 10.1061/(ASCE)GT.1943-5606.0001177, 04014071.
Xiao, Y., Liu, H., Chen, Y., Jiang, J., and Zhang, W. (2014b). "State-dependent constitutive model for rockfill materials." *Int. J. Geomech.*, 10.1061/(ASCE)GM.1943-5622.0000421, 04014075.
Xiao, Y., Liu, H., Desai, C., Sun, Y., and Liu, H. (2016b). "Effect of intermediate principal-stress ratio on particle breakage of rockfill material." *J. Geotech. Geoenviron. Eng.*, 10.1061/(ASCE)GT.1943-5606, 06015017.
Xiao, Y., Liu, H., Liu, H., Chen, Y., and Zhang, W. (2016c). "Strength and dilatancy behaviors of dense modeled rockfill material in general stress space." *Int. J. Geomech.*, 10.1061/(ASCE)GM.1943-5622, 04016015.
Xu, B., Zou, D. G., Kong, X., Hu, Z., and Zhou, Y. (2015). "Dynamic damage evaluation on the slabs of the concrete faced rockfill dam with the plastic-damage model." *Comput. Geotech.*, 65(65), 258–265.
Xu, B., Zou, D. G., and Liu, H. B. (2012). "Three-dimensional simulation of the construction process of the Zipingpu CFRD based on a generalized plasticity model." *Comput. Geotech.*, 43(6), 143–154.
Zhang, C. (2007). "Challenges of high dam construction to computational mechanics." *Front. Archit. Civil Eng. China*, 1(1), 3–43.
Zhong, H., Lin, G., Li, X., and Li, J. (2011). "Seismic failure modeling of concrete dams considering heterogeneity of concrete." *Soil Dyn. Earthquake Eng.*, 31(12), 1678–1689.
Zhu, W. C., and Tang, C. A. (2002). "Numerical simulation on shear fracture process of concrete using mesoscopic mechanical model." *Constr. Build. Mater.*, 16(8), 453–463.
Zienkiewicz, O. C., Leung, K. H., and Pastor, M. (1985). "Simple model for transient soil loading in earthquake analysis. I. Basic model and its application." *Int. J. Numer. Anal. Methods Geomech.*, 9(5), 453–476.
Zou, D. G., Xu, B., Kong, X. J., Liu, H. B., and Zhou, Y. (2013). "Numerical simulation of the seismic response of the Zipingpu concrete face rockfill dam during the Wenchuan earthquake based on a generalized plasticity model." *Comput. Geotech.*, 49(4), 111–122.